

## Photocatalytic study of organosilane-modified zinc oxide nanoparticles

Aurel TĂBĂCARU,\* Mariana BUȘILĂ, Viorica (GHISMAN) PLEȘCAN and Viorica MUȘAT\*

*Center of Nanostructures and Functional Materials – CNMF, Faculty of Engineering, “Dunărea de Jos”  
University of Galați, 111 Domneasca Street, 800201, Galați, Romania*

**Abstract.** In our recent studies, we have investigated the tunability of optical properties of zinc oxide nanoparticles (ZnO NPs) through surface modification with organosilane surfactants. In the present paper, the effect of ZnO NPs modified with variable amount of 3-(trimethoxysilyl)propylmethacrylate (MPS) surfactant was investigated toward the photocatalytic degradation of methylene blue (MB), using two different UV light sources emitting at 254 nm and 365 nm. While the maximum photodegradation efficiency of 63% was reached by ZnO NPs loaded with the highest concentration of MPS upon exposure at 254 nm, in the case of UV exposure at 365 nm an opposite photodegradation trend was observed. Actually, a significant photodegradation efficiency of 95% was recorded by the unmodified ZnO, followed by ZnO NPs modified with 2% MPS for which the photodegradation efficiency amounted to 80%, thus highlighting their best photocatalytic performance.

**Keywords:** zinc oxide nanoparticles, photocatalysis, photodegradation efficiency, methylene blue.

### 1. Introduction

Zinc oxide is an n-type II-VI semiconductor with a wide band gap of 3.37 eV [1], a high exciton binding energy of 60 meV at room temperature [2], good transparency, high electron mobility and room-temperature photoluminescence [3]. These features make this material very favorable for emerging applications in, *e.g.*, optoelectronics [4], UV lasers and photodetectors [5], solar cells [6], thin film transistors [7], gas sensing [8], catalysis [9], cell labeling [10], and even in medical field as antibacterial agents [11] or in naval area as antifouling coatings [12].

One major problem of global concern is related to wastewater treatment, which could be reasonably solved by means of photocatalysis. This recent technology has been adopted as a more efficient and alternative way to activated carbon and biological methods for wastewater treatment. Nanocrystalline TiO<sub>2</sub> and ZnO semiconductors were found to be the most attractive candidates for wastewater treatment, and are well known for their photocatalytic activity, chemical stability, lower cost, easy availability, and strong oxidative capacity [13, 14].

The utilization of such metal oxide based semiconductors materials for the degradation and complete mineralization of a wide range of organic compounds, such as dyes, phenols and pharmaceutical drugs, has already produced several promising results [15-17]. Due to the increasing demands for TiO<sub>2</sub> in the last few years, its

commercialization value has raised, thus exceeding the value of ZnO [18], and therefore, the latter has been chosen as a more suitable alternative resource for TiO<sub>2</sub> in terms of efficiency, cost-effectiveness and environment-friendliness. Actually, due to higher quantum efficiency and low cost of production, ZnO is considered to possess a more efficient photocatalytic activity compared to TiO<sub>2</sub>, though having comparable intrinsic band gap energy [19, 20].

A crucial shortcoming that arises when adopting ZnO NPs in photocatalysis is their tendency to agglomerate due to large surface area and high surface energy. This makes more difficult their utilization in the form of very small nanoparticles, and therefore, it is of demanding importance to control their particles size and surface properties. In this regard, recent researches have revealed on the improvement of photocatalytic activity of ZnO NPs by means of their modification through cationic or anionic doping or by means of adding metals or non-metals [21-23]. Doping ZnO with coinage metals such as silver or gold has shown enhanced photocatalytic activity of the resulting ZnO nanocomposites due to improved charge separation and reduction in electron-hole recombination [24-26].

In our recent investigations, ZnO NPs were modified with organosilane surfactants such as 3-(trimethoxysilyl)propylmethacrylate (MPS) [27] and vinyltrimethoxysilane (VTMS) [28], or with a diquaternary salt of bis(pyridinium) such as N,N'-

\*Corresponding authors: aurel.tabacaru@ugal.ro; viorica.musat@ugal.ro

di(*p*-methoxyphenacyl)-1,2-bis(4-pyridinium)ethane (DSB) [29], and the influence of particles size on the optical properties was studied. In the present contribution, we sought to study the photocatalytic activity, though very less explored, of organo-modified ZnO NPs. Therefore, the effect of ZnO NPs modified with variable amounts of MPS, with different sizes, was investigated toward the photocatalytic degradation of methylene blue (MB) in aqueous solution, using two different UV light sources emitting at 254 nm and 365 nm.

## 2. Experimental

### 2.1. Synthesis of organosilane-modified ZnO NPs

The organosilane-modified ZnO NPs were prepared according to the precipitation method reported in the literature [27]. The obtained samples are hereafter labeled with ZnO for the unmodified nanoparticles, and ZnO-MPS-x% for ZnO NPs modified with 2, 5 and 10% MPS, respectively.

### 2.2. Nanoparticles characterization

The X-ray powder diffraction (XRD) patterns of the obtained nanoparticles were recorded on unoriented ground powders with a DRON-3 diffractometer with a Co K $\alpha$  ( $\lambda = 1.79 \text{ \AA}$ ) radiation, between 10 and 60° 2 $\theta$  degrees with a step size of 0.02°. The diffractograms represented in Fig. 1 were however obtained after applying the conversion factors from Co K $\alpha$  to Cu K $\alpha$  radiation of the 2 $\theta$  values. The average crystallite size ( $L$ ) of synthesized ZnO NPs was estimated by applying the Debye-Scherrer's Eq. (1) [30]:

$$B(2\theta) = \frac{K \cdot \lambda}{L \cdot \cos\theta} \quad (1)$$

where  $B$  is the full width at half the maximum intensity (FWHM),  $\lambda$  is the X-ray wavelength,  $\theta$  is the diffraction angle and  $K$  is the Scherrer's constant whose value for spherical particles is 0.89 [31].

Scanning electron microscopy (SEM) images were collected on a Quanta 200 scanning electron microscope operating at 15 kV. Specimens were prepared by dispersing the samples by sonication in methanol and by depositing few drops of the suspensions on carbon-coated grids.

### 2.3. Photocatalytic measurements

The photocatalytic activity of ZnO NPs was evaluated through the bleaching of methylene blue (MB) aqueous solution (20 mL, 0.1%) in the presence of 0.05 g powder of investigated nanoparticles, under UV illumination at both 254 nm and 365 nm for 60 min.

The bleaching of MB aqueous solution was quantitatively measured by UV-Vis absorption spectra performed with a Microplate reader with

fluorescence spectrometer Infinite 200 PRO NanoQuant (Tecan, Switzerland), in the 400–800 nm range.

The photocatalytic activity of the prepared ZnO photocatalysts was quantitatively evaluated by determining the photodegradation efficiency ( $\eta\%$ ) of methylene blue with Eq. (2):

$$\eta = \frac{A_0 - A}{A_0} \cdot 100 \quad (2)$$

where  $A_0$  is the absorbance of the dye-containing solutions before UV illumination and  $A$  is the absorbance of the same solutions after UV illumination.

## 3. Results and Discussions

### 3.1. Morpho-structural characterization of ZnO NPs

The XRPD patterns of all samples (Fig. 1) show the three main diffraction peaks located in the 30 – 40° 2 $\theta$  range, assignable to the (100), (002) and (101) planes that are specific for zinc oxide wurtzite structure [32]. Worthy of note, the diffraction pattern of unmodified ZnO NPs shows well resolved reflections, while a broadening of the diffraction peaks are observed in the case of MPS-modified ZnO NPs, thus indicating a progressive reduction of their crystallinity along with the size reduction induced through organosilane surface modification.

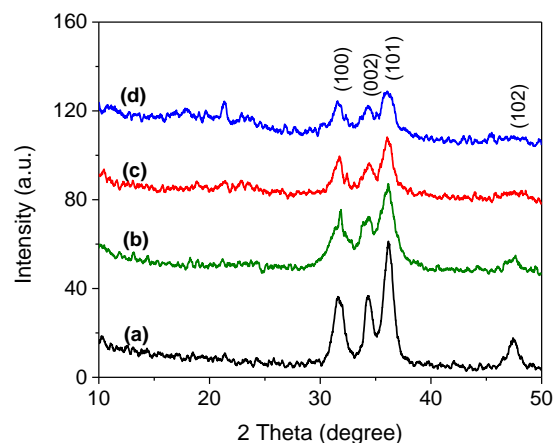


**Figure 1.** XRPD profiles of ZnO (a), ZnO-MPS-2% (b), ZnO-MPS-5% (c), and ZnO-MPS-10% (d).

The average crystallite size of prepared ZnO NPs was estimated by applying the Debye-Scherrer's Eq. (1), and a progressive decrease of the crystallite size from 9.5 nm for ZnO to 7, 6.5 and 3 nm for ZnO-MPS-2%, ZnO-MPS-5% and ZnO-MPS-10%, respectively, was attained.

Particle size and morphology of ZnO samples were also studied by scanning electron microscopy (SEM) and their micrographs are given in Fig. 2.

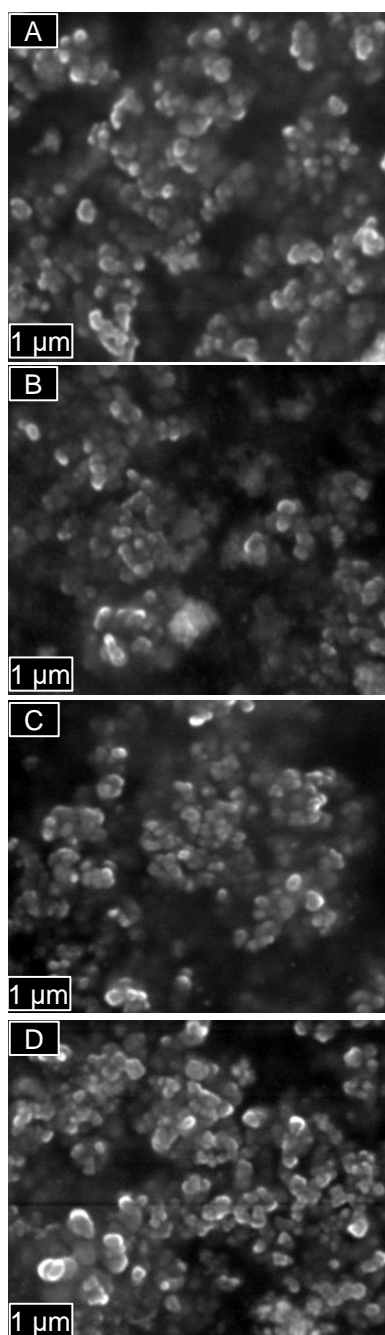


**Figure 2.** SEM images of ZnO (A), ZnO-MPS-2% (B), ZnO-MPS-5% (C) and ZnO-MPS-10% (D).

The SEM image of unmodified ZnO sample (Fig. 2A) shows that this material consists of primary particles of *ca.* 29 nm with nearly spherical shape that are mostly organized into bigger agglomerates. Particles with similar morphology are also observed for all the organosilane-treated ZnO samples. In the case of ZnO-MPS 2% (Fig. 2B), the primary particles have diameters of *ca.* 23 nm and are fused into bigger agglomerates, which in turn are fused into even bigger aggregates. The primary particles become smaller as the organosilane concentration increases, and thus sizes of *ca.* 11 nm

for ZnO-MPS 5% (Fig. 2C) and *ca.* 6 nm for ZnO-MPS 10% (Fig. 2D) are attained.

### 3.2. Photocatalytic activity

Two series of experiments were carried out by exposing the methylene blue (MB) aqueous solutions containing the prepared ZnO NPs at two UV irradiation wavelengths, 254 nm and 365 nm. In Fig. 3, the absorbance spectra of both MB solution and ZnO NPs based MB solutions, after exposure at 254 nm for one hour, are given. From this figure, it can be observed that the extent of photocatalytic degradation of MB is determined by the reduction of the absorbance of all MB solutions containing ZnO NPs (the maximum peak was observed at  $\lambda_{\max} = 665$  nm), with a decreasing trend from unmodified ZnO to ZnO-MPS-10%. The values of their absorbance is comprised in a very narrow range, especially for ZnO NPs modified with 2% and 5% MPS, whose absorbance spectra are completely overlapped. The decreased values of the absorbance is in direct correlation with the rate of discoloration, which increased as the nanoparticles size decreased.

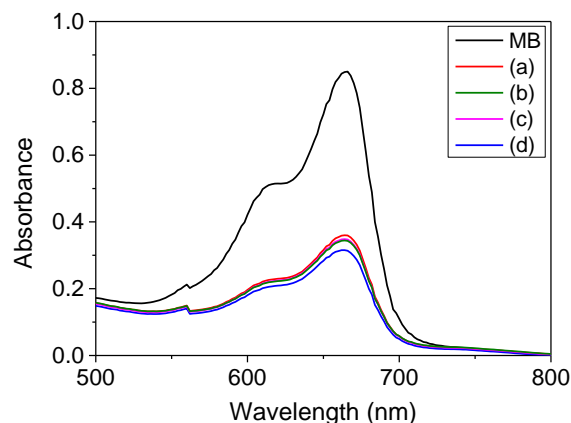


**Figure 3.** UV-Vis absorption spectra of methylene blue in the presence of ZnO (a), ZnO-MPS-2% (b), ZnO-MPS-5% (c) and ZnO-MPS-10% (d), after UV irradiation at 254 nm.

As indicated in Fig. 4, the photodegradation efficiency of all ZnO samples has greatly enhanced, though being comprised in a very narrow range, increasing from 58% in unmodified ZnO to 63% in ZnO-MPS-10%. Thus, the photocatalytic reaction rates of these nanoparticles could be enhanced by maneuvering their particles size to improve the electron transfer rates [33].

In Fig. 5, the absorbance spectra of both MB solution and ZnO NPs based MB solutions, after exposure at 365 nm for one hour, are given. From this figure, the extent of photocatalytic degradation of MB is evidenced by the reduction of the absorbance of all MB solutions containing ZnO NPs. Even in this case, the maximum peak was observed at  $\lambda_{\max} = 665$  nm. Unlike the first series of

experiments, the variation trend of the absorbance values observed in the second series of experiments was opposite. As such, the absorbance values decreased from ZnO-MPS-10% to unmodified ZnO NPs, and the rate of discoloration decreased as the nanoparticles size increased.

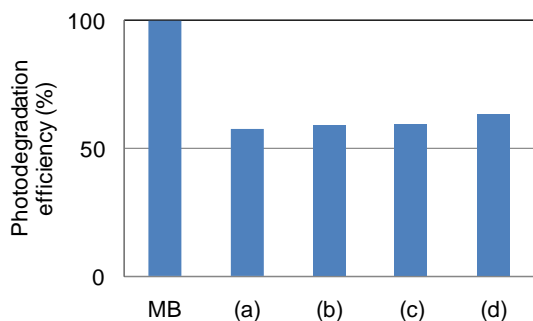


**Figure 4.** Photodegradation efficiency of ZnO (a), ZnO-MPS-2% (b), ZnO-MPS-5% (c) and ZnO-MPS-10% (d), after UV exposure of MB-containing solutions at 254 nm.

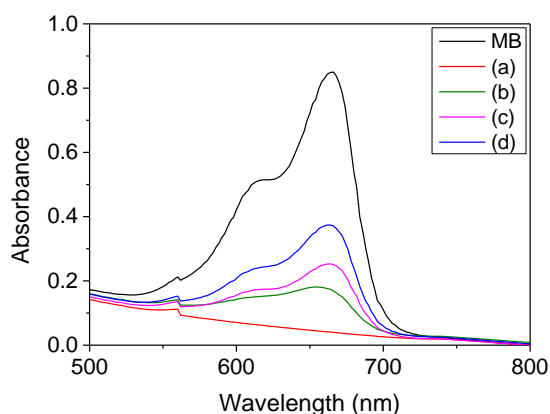


**Figure 5.** UV-Vis absorption spectra of methylene blue in the presence of ZnO (a), ZnO-MPS-2% (b), ZnO-MPS-5% (c) and ZnO-MPS-10% (d), after UV irradiation at 365 nm.

As indicated in Fig. 6, the photodegradation efficiency of all ZnO samples increased from 56% in the case of ZnO-MPS-10% to 70%, 80% and 95% for ZnO-MPS-5%, ZnO-MPS-2% and unmodified ZnO, respectively. As a matter of fact, a complete discoloration of unmodified ZnO NPs based MB solution was observed (Fig. 7), thus highlighting the best photocatalytic performance exhibited by the unmodified ZnO NPs towards the degradation of MB molecules upon UV exposure at 365 nm for 1 h. A comparable performance was also attained by Chiu *et al.* on two-dimensional ZnO nanopellets upon UV exposure at 254 nm for 6 h [34], and by Musat *et al.* on ZnO NPs with nanocrystallites size of 7 nm upon exposure at 210 nm for 1 h [35].

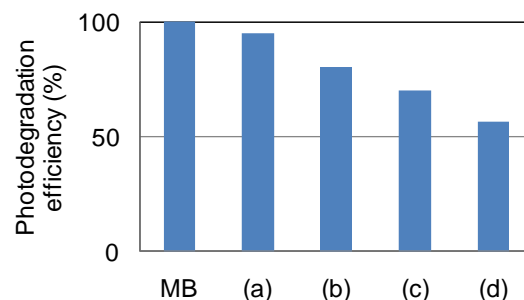


**Figure 6.** Photodegradation efficiency of ZnO (a), ZnO-MPS-2% (b), ZnO-MPS-5% (c) and ZnO-MPS-10% (d), after UV exposure of MB-containing solutions at 365 nm.

As far as the photocatalytic activity of ZnO NPs modified with MPS is concerned, the values obtained for the photodegradation efficiency are also significant, especially for ZnO samples modified with 2% and 5% MPS upon UV exposure at 365 nm. To the best of our knowledge, no other report, where ZnO NPs were found to exhibit enhanced photodegradation efficiency after being modified with this type of organosilane surfactant, was found up to date. Instead, in only one report ZnO NPs modified with polystyrene were studied for the photocatalytic degradation of methylene orange, and for this case, the organic surfactant induced a significant decrease in the photodegradation efficiency in comparison with unmodified ZnO NPs which proved much more effective [36]. This fact allows us to state that only a limited number of organic surfactants are able to produce a positive influence on the photocatalytic performance in the modified ZnO NPs.

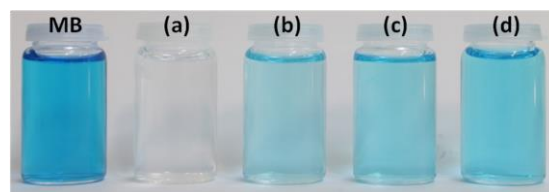


**Figure 7.** Color of the methylene blue solution before UV irradiation (MB) and discoloration of MB solutions containing ZnO (a), ZnO-MPS-2% (b), ZnO-MPS-5% (c) and ZnO-MPS-10% (d), after UV irradiation at 365 nm.

The different behavior of this series of nanoparticles at the two UV exposure wavelengths of 254 nm and 365 nm could be explained not only on the basis of nanoparticles size, but also on the effect of chemical groups present in the structure of the organosilane surfactant. On the other hand, the energy corresponding to the wavelength of 254 nm is too high to be absorbed by the ZnO-MPS samples, making the organosilane shell, which surrounds the ZnO core [27], to act like a barrier against UV radiation. Consequently, the partial coverage of ZnO

surface with this organosilane allows less generation of hydroxyl radicals for the oxidation of MB molecules, thus leading to lower photodegradation efficiency of MPS-modified ZnO samples. The energy corresponding to the wavelength of 365 nm, instead, is sufficiently low to promote the absorption on behalf of the ZnO-MPS samples. In this case, the barrier effect of the organosilane shell is cancelled, thus allowing a better generation of hydroxyl radicals to oxidize much higher amount of MB molecules. These aspects, along with the photocatalytic mechanism related to such type of organosilane-modified ZnO NPs, will be developed in more detail in the near future study.

#### 4. Conclusions

The photocatalytic performance of a series of ZnO NPs modified with the organosilane surfactant MPS was tested towards the degradation of MB at two UV exposure wavelengths. Modification of ZnO surface was found to have a great influence on its photocatalytic activity. The optimal condition for the photocatalytic degradation of MB using this series of ZnO NPs was their exposure at 365 nm for 1 h. The best photocatalyst was the unmodified ZnO, reaching a photodegradation efficiency of 95%, followed by ZnO NPs modified with 2% MPS for which the photodegradation efficiency amounted to 80%. These results are of great importance for solving, *e.g.*, the issues of worldwide concern, such as quality drinking water, wastewater treatment and bacteria disinfection.

#### Acknowledgments

The work of Aurel Tăbăcaru has been funded by the Sectoral Operational Program Human Resources Development 2007-2013 of the Ministry of European Funds through the Financial Agreement POSDRU/159/1.5/S/132397. Prof. Rodica Dinica from the "Dunărea de Jos" University of Galati is gratefully acknowledged for helpful experimental assistance.

#### References

- [1]. M.A. Hood, M. Mari, R. Muñoz-Espí, *Materials* **7**, 4057 (2014).
- [2]. J. Li and J.Z. Zhang, *Coord. Chem. Rev.* **253**, 3015 (2009).
- [3]. C.F. Klingshirn, B.K. Meyer, A. Waag, A. Hoffmann and J. Geurts, *Zinc Oxide From Fundamental Properties Towards Novel Applications*, Springer-Verlag, Berlin, 2010.
- [4]. L. Qian, Y. Zheng, J. Xue and P.H. Holloway, *Nature Photonics* **5**, 543 (2011).
- [5]. U. Ozgur, Ya.I. Alivov, C. Liu, A. Teke, M.A. Reshchikov, S. Dogan, V. Avrutin, S.-J. Cho and H. Morkoc, *J. Appl. Phys.* **98**, 041301 (2005).
- [6]. J. Mawyin, Y. Shupyk, M. Wang, G. Poize, P. Atienzar, T. Ishwara, J.R. Durrant, J. Nelson, D. Kanehira, N. Yoshimoto, C. Martini, E. Shilova, P. Secondo, H. Brisset, F. Fages and J. Ackermann, *J. Phys. Chem. C* **115**, 10881 (2011).
- [7]. E. Fortunato, P. Barquinha and R. Martins, *Adv. Mater.* **24**, 2945 (2012).
- [8]. M. Karimi, J. Saydi, M. Mahmoodi, J. Seidi, M. Ezzati, S. Shamsi Anari and B. Ghasemian, *J. Phys. Chem. Solid* **74**, 1392 (2013).
- [9]. Y. Martynova, B.-H. Liu, M.E. McBriarty, I.M.N. Groot, M.J. Bedzyk, S. Shaikhutdinov and H.-J. Freund, *J. Catal.* **301**, 227 (2013).
- [10]. X. Tang, E.S.G. Choo, L. Li, J. Ding and J. Xue, *Langmuir* **25**, 5271 (2009).
- [11]. M. Busila, V. Musat, T. Textor and B. Mahltig, *RSC Adv.* **5**, 21562 (2015).
- [12]. D.M. Yebra, S. Kiil, C.E. Weinell and K. Dam-Johansen, *Prog. Org. Coat.* **56**, 327 (2006).
- [13]. M.R. Hoffmann, S.T. Martin, W. Choi and D.W. Bahnemann, *Chem. Rev.* **95**, 69 (1995).
- [14]. P. Periyat, S.C. Pillai, D.E. McCormack, J. Colreavy and S.J. Hinder, *J. Phys. Chem. C* **112**, 7644 (2008).
- [15]. S. Funk, B. Hokkanen, U. Burghaus, A. Ghicov and P. Schmuki, *Nanoletters* **7**, 1091 (2007).
- [16]. T. Zhang, T. Oyama, S. Horikoshi, J. Zhao, N. Serpone and H. Hidaka, *Appl. Catal. B: Environ.* **42**, 13 (2003).
- [17]. T. Zhang, L. You and Y. Zhang, *Dyes Pigments* **68**, 95 (2006).
- [18]. J. Emsley, *Titanium. Nature's Building Blocks: An A-Z Guide to the Elements*, Oxford University Press, Oxford, England, 2001.
- [19]. S. Sakthivel, B. Neppolian, M.V. Shankar, B. Arabindoo, M. Palanichamy and V. Murugesan, *Sol. Energy Mater. Sol. C* **77**, 65 (2003).
- [20]. J.H. Sun, S.Y. Dong, Y.K. Wang and S.P. Sun, *J. Hazard. Mater.* **172**, 1520 (2009).
- [21]. P.V. Kamat, R. Huehn and R. Nicolaescu, *J. Phys. Chem. B* **106**, 788 (2002).
- [22]. S.C. Padmanabhan, S.C. Pillai, J. Colreavy, S. Balakrishnan, D.E. McCormack, T.S. Perova, S.J. Hinder and J.M. Kelly, *Chem. Mater.* **19**, 4474 (2007).
- [23]. J.M. Herrmann, H. Tahiri, Y. Ait-Ichou, G. Lassaletta, A.R. González-Elipe and A. Fernández, *Appl. Catal. B: Environ.* **13**, 219 (1997).
- [24]. K. Saoud, R. Alsubaihi, N. Bensalah, T. Bora, M. Bertino, J. Dutta, *Mater. Res. Bull.* **63**, 134 (2015).

- [25]. M. Ibanescu (Busila), V. Musat, T. Textor, V. Badilita, B. Mahltig, *J. Alloys Compd.* **610**, 244 (2014).
- [26]. G. Merga, L.C. Cass, D.M. Chipman and D. Meisel, *J. Am. Chem. Soc.* **130**, 7067 (2008).
- [27]. V. Musat, A. Tabacaru, B.S. Vasile and V.-A. Surdu, *RSC Adv.* **4**, 63128 (2014).
- [28]. A. Tabacaru, V. Musat, N. Tigau, B.S. Vasile and V.-A. Surdu, *Appl. Surf. Sci.*, to be published.
- [29]. A. Tabacaru, V. Musat, R.M. Dinica and C. Gheorghies, *Rev. Chim. (Bucharest)*, to be published.
- [30]. A.L. Patterson, *Phys. Rev.* **56**, 972 (1939).
- [31]. H.P. Klug and L.E. Alexander, *X-ray diffraction procedures for polycrystalline and amorphous materials*, Wiley, New York, 1974.
- [32]. Powder Diffract. File, JCPDSB Internat. Centre Diffract. Data, PA 19073–3273, U.S.A. (2001).
- [33]. K.J. Klabunde (Ed.), *Nanoscale Materials in Chemistry*, John Wiley & Sons, Inc., USA, 2002.
- [34]. W.S. Chiu, P.S. Khiew, M. Cloke, D. Isa, T.K. Tan, S. Radiman, R. Abd-Shukor, M.A. Abd. Hamid, N.M. Huang, H.N. Limd and C.H. Chia, *Chem. Eng. J.* **158**, 345 (2010).
- [35]. M. (Busila) Ibanescu, V. Musat, T. Textor, V. Badilita, B. Mahltig, *The Annals of "Dunarea de Jos" of Galati, Fascicle IX, Metallurgy and Materials Science* **2**, 54 (2013).
- [36]. R.Y. Hong, J.H. Li, L.L. Chen, D.Q. Liu, H.Z. Li, Y. Zheng and J. Ding, *Powder Technology* **189**, 426 (2009).

*Received:* 17 September 2015

*Received in revised form:* 21 September 2015

*Accepted:* 21 September 2015